Fra-2/AP-1 controls bone formation by regulating osteoblast differentiation and collagen production

Aline Bozec,[1] Latifa Bakiri,[1] Maria Jimenez,[1] Thorsten Schinke,[2] Michael Amling,[2] and Erwin F. Wagner[1]

[1]Genes, Development, and Disease Group, BBVA Foundation, Cancer Cell Biology Program, Spanish National Cancer Center, E-28029 Madrid, Spain
[2]Department of Osteology and Biomechanics, University Medical Center Hamburg-Eppendorf, D-20246 Hamburg, Germany

The activator protein-1 (AP-1) transcription factor complex, in particular the Fos proteins, is an important regulator of bone homeostasis. Fra-2 (*Fosl2*), a Fos-related protein of the AP-1 family, is expressed in bone cells, and newborn mice lacking Fra-2 exhibit defects in chondrocytes and osteoclasts. Here we show that Fra-2–deficient osteoblasts display a differentiation defect both in vivo and in vitro. Moreover, Fra-2–overexpressing mice are osteosclerotic because of increased differentiation of osteoblasts, which appears to be cell autonomous. Importantly, the osteoblast-specific *osteocalcin* (*Oc*) gene and *collagen1α2* (*col1α2*) are transcriptional targets of Fra-2 in both murine and human bone cells. In addition, Fra-2, Oc, and col1 are expressed in stromal cells of human chondroblastic and osteoblastic osteosarcomas (Os's) as well as during osteoblast differentiation of human Os cell lines. These findings reveal a novel function of Fra-2/AP-1 as a positive regulator of bone and matrix formation in mice and humans.

Introduction

Bone remodeling is a process of continuous resorption and neosynthesis of bone that determines bone structure and quality during adult life. Osteoblasts, the bone-forming cells, can regulate osteoclast formation by expressing the negative regulator osteoprotegerin (OPG) or positive regulators, such as receptor activator of NF-κB ligand (Rankl) and macrophage colony–stimulating factor 1 (Teitelbaum and Ross, 2003; Takeda and Karsenty, 2008). Imbalances in bone remodeling can result in severe perturbations in skeletal structure and function, leading to conditions such as osteoporosis, osteosclerosis, and osteopetrosis. Osteoporosis is a bone disease in which the bone mineral density is reduced, the bone microarchitecture is disrupted, and the amount of noncollagenous proteins in bone is altered, leading to an increased risk of fractures (Chien and Karsenty, 2005). Osteopetrosis is a disease in which the bones are more brittle as a result of decreased osteoclast function despite increased bone mass (Rodan and Martin, 2000). In contrast, osteosclerosis is a bone disorder characterized by an abnormal hardening and progressive increase in bone mass of the skeleton, resulting from increased bone formation (Rodan and Martin, 2000). Unlike osteopetrosis, the primary defect of this disorder, causing increased bone mass, results from altered osteoblast function. Several soluble molecules and transcription factors, including *Ihh*, *FGF18*, *Runx2*, and *osterix* (*Osx*), regulate osteoblast differentiation (Karsenty and Wagner, 2002). However, the transcriptional mechanisms responsible for the expression of bone-specific genes, in particular extracellular matrix components, are still not fully understood.

The activator protein-1 (AP-1) transcription factor complex consists of a large variety of dimers composed of members of the Fos, Jun, and activating transcription factor (ATF) families (Wagner and Eferl, 2005). AP-1 activity is implicated in a wide range of biological processes, and AP-1 proteins have important roles as regulators of bone development. Loss- and gain-of-function mutations in mice of Fos members, and to a lesser extent of Jun and ATF members, most notably affect chondrocyte, osteoblast, and osteoclast physiology, resulting in a variety of pathological skeletal conditions (Wagner and Eferl, 2005). Chondrocyte-specific inactivation of c-Jun leads to severe scoliosis

Correspondence to Erwin F. Wagner: ewagner@cnio.es

Abbreviations used in this paper: ATF, activating transcription factor; *Bsp*, *bone sialoprotein*; ChIP, chromatin immunoprecipitation; CT, computed tomography; H&E, hematoxylin and eosin; *ko*, *knockout*; Mgp, matrix gla-protein; Oc, osteocalcin; OPG, osteoprotegerin; *Opn*, *osteopontin*; Os, osteosarcoma; *Osx*, *osterix*; qPCR, quantitative PCR; Rankl, receptor activator of NF-κB ligand; SAOs, sarcoma osteogenics; shRNA, short hairpin RNA; tg, transgenic; TRAP, tartrate-resistant acid phosphatase; wt, wild type.

The Rockefeller University Press $30.00
J. Cell Biol. Vol. 190 No. 6 1093–1106
www.jcb.org/cgi/doi/10.1083/jcb.201002111

caused by failure of intervertebral disc formation, suggesting that c-Jun is a regulator of sclerotomal differentiation (Behrens et al., 2003). Moreover, *c-Jun* is essential for efficient osteoclastogenesis (David et al., 2002), whereas conditional loss of *JunB* results in severe osteopenia because of cell-autonomous osteoblast and osteoclast defects (Kenner et al., 2004). Mice lacking *JunD* exhibit increased bone mass as a result of increased bone formation (Kawamata et al., 2008). Mice carrying a germline mutation in ATF-2 display defects in endochondral ossification at epiphyseal plates similar to human hypochondroplasia (Reimold et al., 1996). In addition, ATF-4 was identified as a critical regulator of osteoblast function. It is required for osteoblast-specific expression of *osteocalcin* (*Oc*) and for posttranscriptional regulation of *type I collagen* (*col1*) synthesis, the main constituents of bone matrix, as well as for transcriptional control of *Rankl* expression (Yang et al., 2004; Elefteriou et al., 2005).

Detailed analyses of transgenic (tg) mice overexpressing Fos proteins have underlined the important functions of Fos/AP-1 in osteoblasts. Fos overexpression leads to osteosarcomas (Os's), a bone tumor characterized by transformation of cells of the osteoblastic lineage (Grigoriadis et al., 1993). Moreover, mice overexpressing either the Fos target gene, Fra-1, also known as *Fos-like antigen 1* (*Fosl1*), or the short isoform of FosB, ΔFosB, develop osteosclerosis as a result of enhanced osteoblast differentiation (Jochum et al., 2000; Sabatakos et al., 2000; Kveiborg et al., 2002). We have previously shown that mice lacking Fra-2 (*Fos-like antigen 2* [*Fosl2*]) display deficiencies in chondrocytes (Karreth et al., 2004). In addition, in the absence of Fra-2, the survival of osteoclasts is affected, leading to the formation of giant osteoclasts by a novel pathway (Bozec et al., 2008).

The function of Fra-2 in bone-forming osteoblasts was analyzed in postnatal development and adult bones using *Fosl2 knockout* (*Fosl2 ko* or *Fosl2*$^{-/-}$) pups and *Fosl2 tg* mice (Karreth et al., 2004; Bozec et al., 2008; Eferl et al., 2008). The *Fosl2 tg* mice develop pulmonary fibrosis around 16 wk of age caused by vascular remodeling and subsequent pulmonary fibrosis (Eferl et al., 2008). Interestingly, *Fosl2 tg* mice also develop an osteosclerotic phenotype as early as 4 wk of age by affecting osteoblast differentiation in vivo and in vitro. Moreover, *Fosl2*$^{-/-}$ osteoblasts fail to differentiate in vitro and acquire an adipogenic phenotype. At the molecular level, we demonstrate that in both mouse and human bone cells, osteoblast differentiation is affected likely as a result of reduced expression of *collagen1α2* (*col1α2*) and *Oc*, which are shown to be direct transcriptional targets of Fra-2.

Results

Fosl2 ko pups are osteopenic

To obtain functional data for a role of Fra-2 in osteoblasts, *Fosl2 ko* pups were analyzed (Karreth et al., 2004; Eferl et al., 2007; Bozec et al., 2008). Von Kossa staining and quantitative histomorphometry revealed a 50% decrease of mineralized bone as well as a 40% decrease in calvarial thickness, whereas osteoblast numbers were not altered (Fig. 1 A; Bozec et al., 2008). We next performed molecular analyses of osteoblast markers by quantitative PCR (qPCR) and in situ hybridization using *Fosl2*$^{-/-}$ newborn mice. Increased expression of *osteopontin (Opn)*, an early osteoblast, late chondrocyte, but also osteoclast marker, was observed in *Fosl2 ko* bone at P2 (day 2 after birth). Moreover, a reduction of *Runx2*, *bone sialoprotein* (*Bsp*), *col1α2*, and *Oc* expression, late markers of osteoblast function, was observed (Fig. 1 B). Osteoblast marker genes, such as *ATF-4*, *osteonectin*, *Osx*, *OPG*, *Rankl*, *col1α1*, and *matrix gla-protein* (*Mgp*), were unaffected (Fig. 1 B). Consistent with lower Oc expression, Oc secretion was also significantly reduced in sera from P2 pups (unpublished data). The increase in *Opn* mRNA levels and the reduction of *Runx2*, *Bsp*, *col1α2*, and *Oc* mRNA expression were confirmed by in situ hybridization (Fig. 1 C). As osteoblasts and adipocytes are derived from common progenitor cells, we quantified the numbers of adipocytes in *Fosl2*$^{-/-}$ and *Fosl2*$^{+/+}$ long bones at P2. No significant changes between the two genotypes were observed (Fig. 1 D). Next we analyzed early and late adipocyte markers by qPCR to assess a potential differentiation defect. *Adipocyte protein* (*Ap-2*), *preadipocyte factor 1* (*Pref1*), and *glucose transporter 4* (*Glut4*) mRNA were found to be unaffected. However, *CCAAT/enhancer binding protein-α* (*CEBP-α*), *CCAAT/enhancer binding protein-β* (*CEBP-β*), and *peroxisome proliferator-activated receptor-γ* (*PPAR-γ*) mRNA expression was increased (Fig. 1 E), suggesting an effect on adipocyte differentiation in vivo.

Osteoblast differentiation defects in the absence of Fra-2 in vitro

To investigate a possible cell-autonomous defect leading to osteopenia in *Fosl2 ko* pups, the activity of osteoblasts was analyzed in vitro. Primary osteoblasts were prepared from calvariae of neonatal mice and differentiated in vitro. Staining for osteoblast differentiation markers, such as *AP*, revealed no major differences in *Fosl2 ko* cells (unpublished data). The activity of osteoblasts was next analyzed by the deposition of mineralized extracellular matrix. The deposition of mineralized extracellular matrix was reduced as shown by Alizarin red staining and by quantification of the number of mineralized nodules (Fig. 2 A). Similar results were observed when osteoblasts were differentiated from bone marrow stromal cells. Importantly, Oil red O staining for mature adipocytes and quantification of the number of adipocytes revealed a significant increase in *Fosl2 ko* cells (Fig. 2 A). Interestingly, expression levels of transcripts for *Runx2*, *col1α2*, and *Oc* were decreased at day 10 and 15 in *Fosl2 ko* cells, whereas mRNA expression for *ATF-4*, *Osx*, and *col1α1* was unaffected (Fig. 2 B). Moreover, the collagen content was found to be decreased in conditioned medium from *Fosl2 ko* cultures (Fig. 2 C). Consistent with the increased numbers of mature adipocytes in *Fosl2 ko* cells, adipocyte markers such as *Ap2*, *Pref1*, *CEBP-α*, *CEBP-β*, and *PPAR-γ* were increased in *Fosl2 ko* cells, whereas *Glut4* expression was unaffected (Fig. 2 B). The proliferation rate of *Fosl2 ko* calvarial osteoblasts, determined by BrdU incorporation, was increased by 50% after 2 d of culture (Fig. 2 D), and growth curve analysis

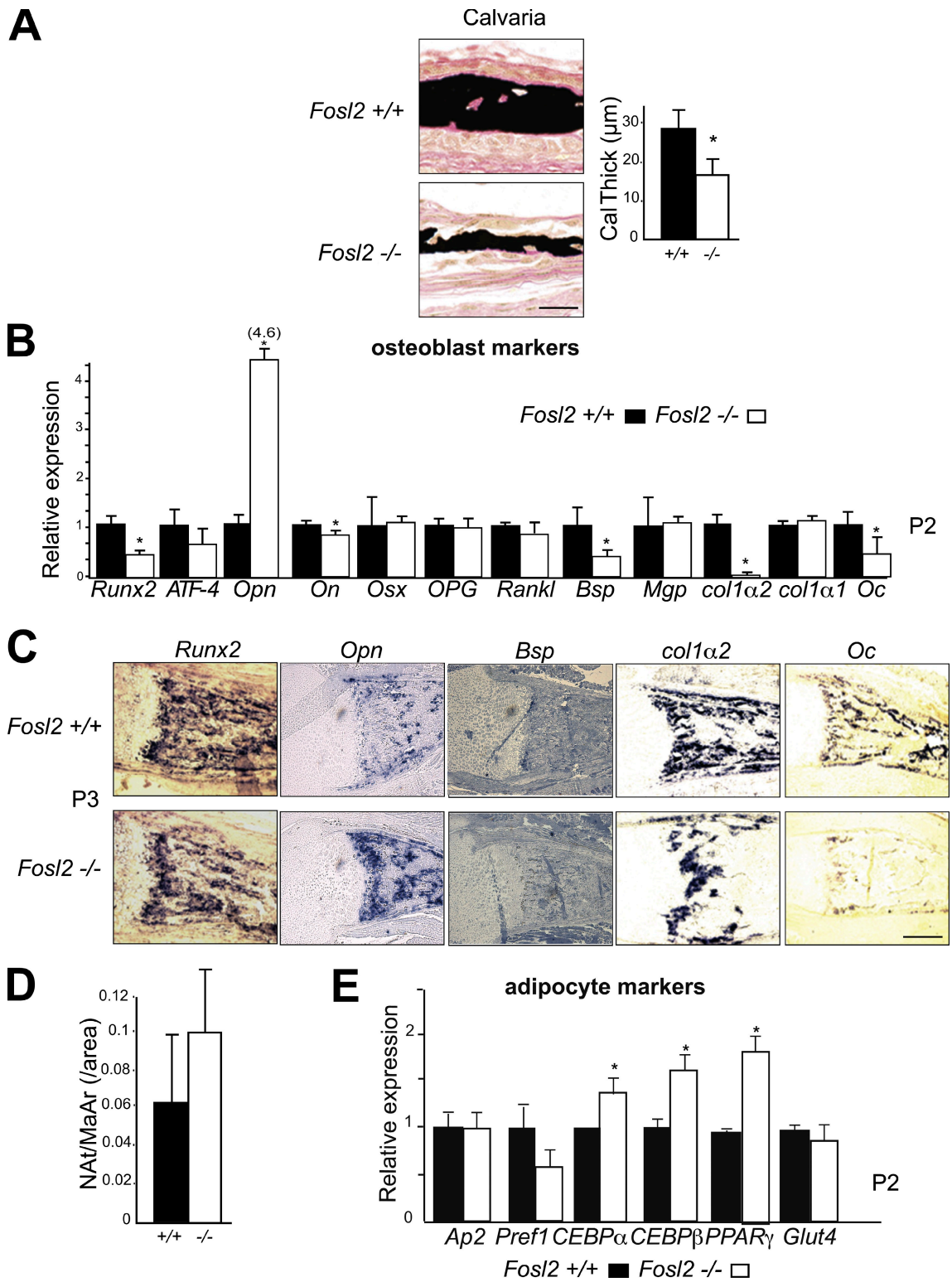

Figure 1. ***Fosl2 ko* pups exhibit an osteopenic phenotype.** (A) Von Kossa staining of calvaria at P3. Quantification of bone volume calvaria thickness (P3; *Fosl2*$^{+/+}$, *n* = 7; *Fosl2*$^{-/-}$, *n* = 6). (B) qPCR analyses of *Runx2*, *ATF-4*, *osteopontin* (*Opn*), *osteonectin* (*On*), *osterix* (*Osx*), *osteoprotegerin* (*OPG*), *receptor activator* of *NF-κB ligand* (*Rankl*), *bone sialoprotein* (*Bsp*), *matrix gla-protein* (*Mgp*), *collagen 1α2* (*col1α2*), *collagen 1α1* (*col1α1*), and *osteocalcin* (*Oc*) in *Fosl2*$^{+/+}$ and *Fosl2*$^{-/-}$ total long bone mRNA at P2. 4.6 represents the relative expression of *Opn* in *Fosl2*$^{-/-}$ long bone. (C) In situ hybridization for *Runx2*, *Opn*, *Bsp*, *col1α2*, and *Oc* on P2 long bones. (D) Quantification of adipocyte numbers (Nat/MaAr) in *Fosl2*$^{+/+}$ and *Fosl2*$^{-/-}$ total long bones (P3; *Fosl2*$^{+/+}$, *n* = 7; *Fosl2*$^{-/-}$, *n* = 6). (E) qPCR analyses of *Adipocyte protein* (*Ap-2*), *preadipocyte factor 1* (*Pref1*), *CCAAT/enhancer binding protein-α* (*CEBP-α*), *CCAAT/enhancer binding protein-β* (*CEBP-β*), *peroxisome proliferator-activated receptor-γ* (*PPAR-γ*), and *glucose transporter 4* (*Glut4*) in *Fosl2*$^{+/+}$ and *Fosl2*$^{-/-}$ total long bone mRNA at P2. Error bars represent mean values ± SD, and wt is set to *, P < 0.01; *Fosl2*$^{+/+}$, *n* = 4 and *Fosl2*$^{-/-}$, *n* = 6. Bars, 500 µm.

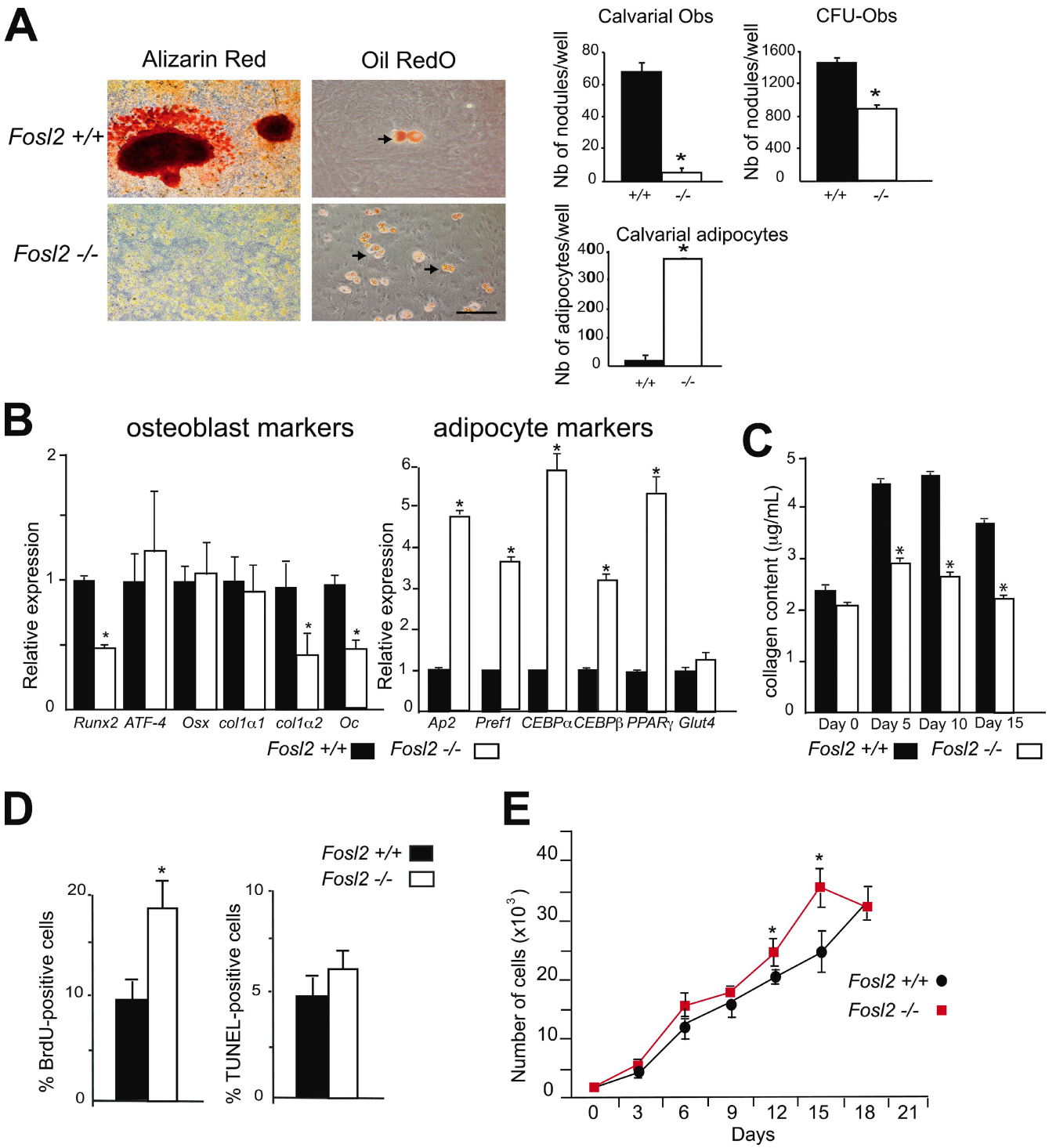

Figure 2. **Osteoblast differentiation of *Fosl2 ko* cells in vitro.** (A) Alizarin red and Oil red O/hematoxylin staining of calvaria-derived osteoblasts isolated from *Fosl2*$^{+/+}$ and *Fosl2*$^{-/-}$ pups. Cells were cultured for 15 d on plastic in the presence of β-glycerophosphate and ascorbic acid. Quantification of the number of nodules and adipocytes per well is shown. Arrows indicate adipocytes. Bars, 200 µm. (B) qPCR analyses of osteoblast markers (*Runx2*, *ATF-4*, *osterix* [*Osx*], *collagen 1α1* [*col1α1*], *collagen 1α2* [*col1α2*], and *osteocalcin* [*Oc*]) and adipocyte markers (*Ap2*, *Pref1*, *CEBP-α*, *CEBP-β*, *PPAR-γ*, and *Glut4* in *Fosl2*$^{+/+}$ and *Fosl2*$^{-/-}$ cells at day 15 of differentiation; $n = 3$). Values are presented as relative expression, and wt is set to 1. (C) Collagen content in *Fosl2*$^{+/+}$ and *Fosl2*$^{-/-}$ osteoblast–conditioned medium at day 0, 5, 10, and 15 of differentiation ($n = 3$). (D) BrdU incorporation and TUNEL-positive cells of calvaria-derived osteoblasts isolated from *Fosl2*$^{+/+}$ and *Fosl2*$^{-/-}$ pups. (E) Cumulative cell number (proliferation) of *Fosl2*$^{+/+}$ and *Fosl2*$^{-/-}$ osteoblasts. *, $P < 0.01$; $n = 3$. Error bars represent mean values ± SD.

showed that cell density and proliferation capacity were slightly increased in *Fosl2 ko* cells (Fig. 2 E). No difference was observed regarding apoptosis of osteoblasts as determined by TUNEL assay after 2 d of culture (Fig. 2 D). These findings indicate that Fra-2 controls osteoblast differentiation and matrix expression in a cell-autonomous manner.

Fosl2 tg mice are osteosclerotic and exhibit altered matrix protein expression

To assess a potential direct effect of Fra-2 on bone-forming cells in adult mice in vivo, histomorphometric and molecular analyses were performed on Fra-2–overexpressing mice (Eferl et al., 2008). No obvious phenotype was observed in *Fosl2 tg* newborns (unpublished data). The bone volume was similar between wild-type (wt) and mutant mice until 2 wk of age, whereas 4-wk- and 3-mo-old mice exhibited an increased bone volume as shown by microcomputed tomography (micro-CT) analysis (Fig. 3, A and B). Histomorphometric analyses on *Fosl2 tg* and control mice at two different time points (4 wk and 3 mo) revealed that bone volume, bone formation, and bone surface were increased in *Fosl2 tg* mice (Fig. 3 B). The number of osteoblasts was significantly increased only in 4-wk-old, but not in 3-mo-old, mice (Fig. 3 B). Interestingly, the number of adipocytes was significantly decreased in *Fosl2 tg* long bones compared with controls at 3 mo of age (Fig. 3 B and Fig. S1 A). Importantly, osteoclast activity, numbers, and size were unchanged as shown by CTx measurements, tartrate-resistant acid phosphatase (TRAP) staining, and histomorphometric analyses (Fig. S1, B and C). Moreover, in vitro osteoclast differentiation revealed no difference on plastic or on dentine slices between control and *Fosl2 tg* cells. The activity of osteoclasts in vitro was increased as shown by resorption markers such as *TRAP*, *CathK*, *MMP9*, *CaII*, and *Nfatc1* (Fig. S1 D). This result is characteristic of an osteosclerotic phenotype accompanied by increased function or differentiation of osteoblasts. Consistent with lower expression of *col1α2* and *Oc* in *Fosl2 ko* long bones, increased expression levels of *col1α2* and *Oc* mRNA were observed in *Fosl2 tg* long bones from 4-wk- and 3-mo-old mice (Fig. 3, C and D). No differences in the levels of *Opn* and *Runx2* mRNA were observed, whereas these markers were affected in *Fosl2 ko* long bones. At 3 mo, the level of *OPG* mRNA was decreased, and the level of *Rankl* mRNA was increased in *Fosl2 tg* long bones (Fig. 3, C and D). However, the levels of OPG and Rankl were unaffected in sera from 3-mo-old *Fosl2 tg* mice (Fig. 3 E). Next, the mRNA levels of adipocyte markers were measured. No difference in the levels of *Pref1*, *CEBP-α*, *CEBP-β*, and *Glut4* mRNA was observed, although the levels of *Ap2* and *PPAR-γ* mRNA were decreased in 3-mo-old *Fosl2 tg* long bones (Fig. 3 F).

Enhanced osteoblast differentiation of *Fosl2 tg* cells in vitro

The cell-autonomous effect of Fra-2 in osteoblast differentiation was next analyzed in *Fosl2 tg* calvarial osteoblasts. Increased deposition of mineralized extracellular matrix and reduced differentiation into adipocytes were observed in *Fosl2 tg* compared with control cells (Fig. 4 A). *Runx2*, *col1α2*, and *Oc* mRNA expression was strongly increased at 10 and 15 d of culture, whereas no differences in the RNA levels of *ATF-4*, *Osx*, and *col1α1* were observed, similar to *Fosl2 ko* cells (Fig. 2 B vs. Fig. 4 B). The expression of adipocyte markers *Ap2*, *Pref1*, *CEBP-α*, and *PPAR-γ* was consistently reduced, whereas the expression of *CEBP-β* and *Glut4* was unchanged (Fig. 4 B). Collagen content measured in conditioned medium from *Fosl2 tg* cells was increased at day 5, 10, and 15 of differentiation (Fig. 4 C). Thus, Fra-2 positively regulates the bone-forming activity of osteoblasts in a cell-autonomous manner.

Col1α2 and Oc are direct transcriptional targets of Fra-2 in osteoblasts

The decreased expression of *Oc* and *col1α2* expression in *Fosl2 ko* newborn osteoblasts and the corresponding increased expression in *Fosl2 tg* osteoblasts suggested that these genes may be direct transcriptional targets of Fra-2. To assess Fra-2 binding to the *Oc* promoter, chromatin immunoprecipitation (ChIP) analysis was performed using Fra-2 antibodies on *Fosl2* control and *ko* primary osteoblasts. Specific primer pairs were used to amplify DNA fragments containing the OSE1 binding site in the *Oc* promoter, which has been shown to bind ATF-4 (Yang et al., 2004). As shown in Fig. 5 A, a Fra-2 antibody specifically immunoprecipitated the *Oc* promoter fragment from wt osteoblast chromatin extracts but not from *Fosl2 ko* cells. No binding of other AP-1 members, such as Fra-1, c-Fos, c-Jun, JunB, and JunD, to the *Oc* promoter could be detected (unpublished data). Moreover, in the absence of Fra-2, ATF-4 binding to the same site was decreased by 50%. This was not the result of a decrease in ATF-4 protein levels because binding of ATF-4 to the promoter of another target gene, *Rankl* (Elefteriou et al., 2005), was unchanged in *Fosl2 ko* cells as well as total ATF-4 protein (Fig. 5, A and B). Interestingly, Fra-2 was not able to bind the *Rankl* promoter, consistent with unaltered expression of *Rankl* in *Fosl2 ko* cells, indicating that the interaction of Fra-2 with ATF-4 was probably specific for the *Oc* promoter. Moreover, immunoprecipitation assays in primary osteoblasts showed that Fra-2 and ATF-4 were able to interact (Fig. 5 B).

Additional ChIP assays were performed with antibodies directed against methylated histone H3 to analyze chromatin modifications on the *Oc* promoter (Fig. 5 C). ChIP and subsequent qPCR analyses of the *Oc* promoter revealed low levels of active (H3K4me3) and repressive (H3K27me3) methylation marks in control cells, consistent with a low transcriptional activity of *Oc* in exponentially growing osteoblasts. However, a striking increase in repressive methylation marks was observed in *Fosl2 ko* osteoblasts, suggesting that the absence of Fra-2 leads to a decreased *Oc* promoter activity marked by the recruitment of repressive methylation marks (Fig. 5, H3K27me3). No changes in methylation marks in the *Rankl* promoter were observed between the two genotypes, consistent with the fact that *Rankl* expression is unaffected in the absence of Fra-2 (Fig. 5 C). Moreover, in DNA cotransfection experiments, ATF-4 and Fra-2 expression vectors, as well as a combination of both, increased the activity of a luciferase reporter containing the Oc promoter (pOG2) fragment (Fig. 5 D). This was not observed with the mutated form of the Oc promoter (pOG2-MUT; Fig. 5 D). Activation of the Oc promoter by DNA cotransfection experiments after Fra-2–specific silencing in primary osteoblasts was performed next. Fra-2 and ATF-4 trans-activated the Oc promoter. Because of the 25% remaining Fra-2 mRNA, low levels of Fra-2 might be sufficient for activation of the promoter by ATF-4 alone (Fig. S2 B). Importantly, an ATF-4–Fra-2 forced dimer (Bakiri et al., 2002) efficiently trans-activated the same

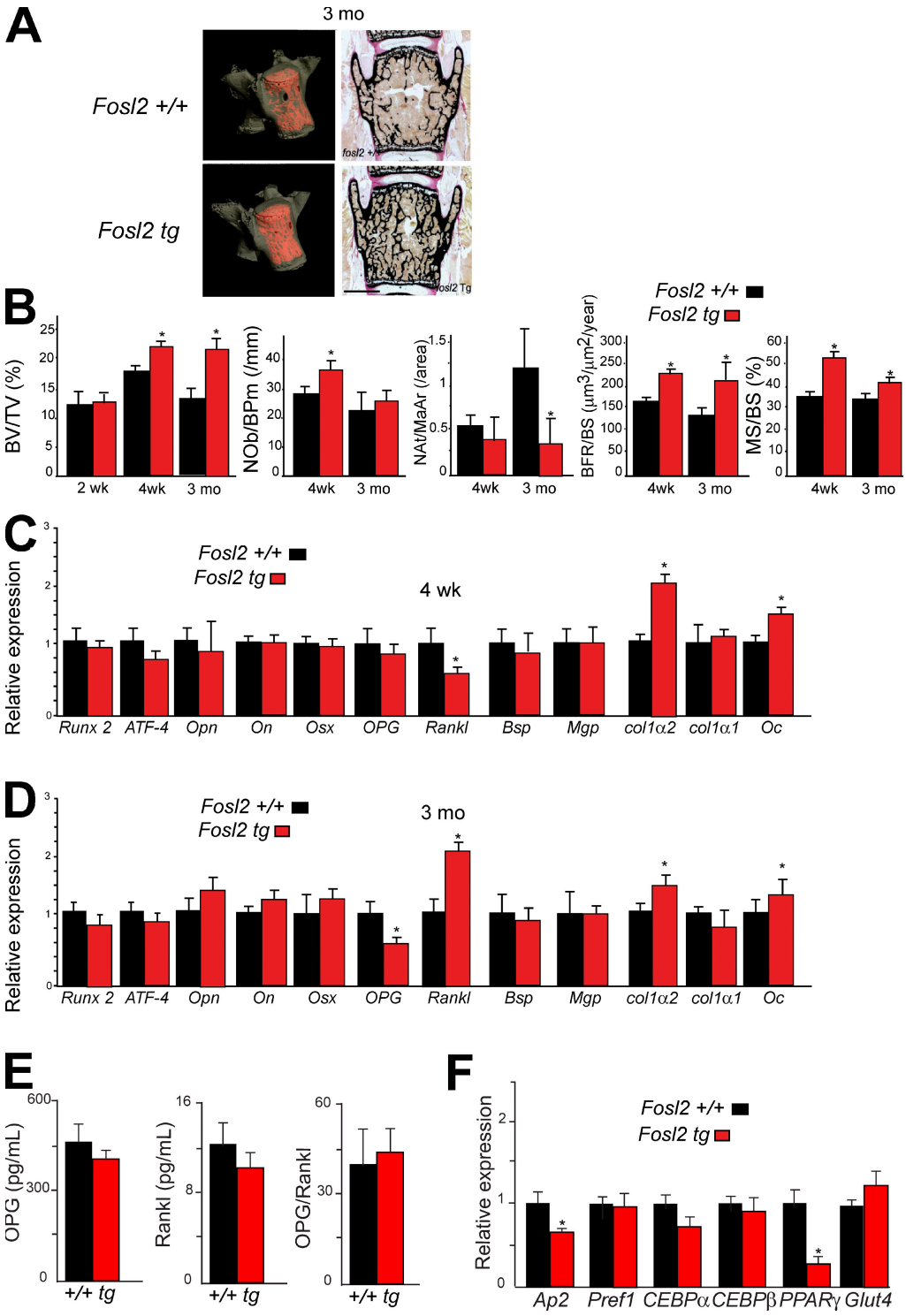

Figure 3. ***Fosl2 tg* mice are osteosclerotic.** (A) Micro-CT and von Kossa staining of spines at 3 mo. Bar, 500 µm. (B) Quantification of bone volume (BV/TV), osteoblast number (Nob/BPm), adipocyte number (Nat/MaAr), bone formation rate (BFR/BS), and bone surface (MS/BS) at 2 wk (n = 4), 4 wk (n = 6/8), and 3 mo (n = 5/8). (C and D) qPCR analyses of *Runx2*, *ATF-4*, *osteopontin* (*Opn*), *osteonectin* (*On*), *osterix* (*Osx*), *osteoprotegerin* (*OPG*), *receptor activator of NF-κB ligand* (*Rankl*), *bone sialoprotein* (*Bsp*), *matrix gla-protein* (*Mgp*), *collagen 1α2* (*col1α2*), *collagen 1α1* (*col1α1*), and *osteocalcin* (*Oc*) in *Fosl2*$^{+/+}$ and *Fosl2 tg* total long bone mRNA at 4 wk (C) and 3 mo (D). wt is set to 1. *, $P < 0.01$; n = 5. (E) OPG and Rankl levels in sera from *Fosl2 wt* and *tg* mice at 3 mo of age (n = 7). The ratio between OPG and Rankl is shown in the third graph. (F) qPCR analyses of *Adipocyte protein* (*Ap-2*), *preadipocyte factor 1* (*Pref1*), *CCAAT/enhancer binding protein-α* (*CEBP-α*), *CCAAT/enhancer binding protein-β* (*CEBP-β*), *peroxisome proliferator-activated receptor-γ* (*PPAR-γ*), and *glucose transporter 4* (*Glut4*) in *Fosl2*$^{+/+}$ and *Fosl2 tg* total long bone mRNA at 3 mo of age. Error bars represent mean values ± SD, and wt is set to *, $P < 0.01$; n = 6.

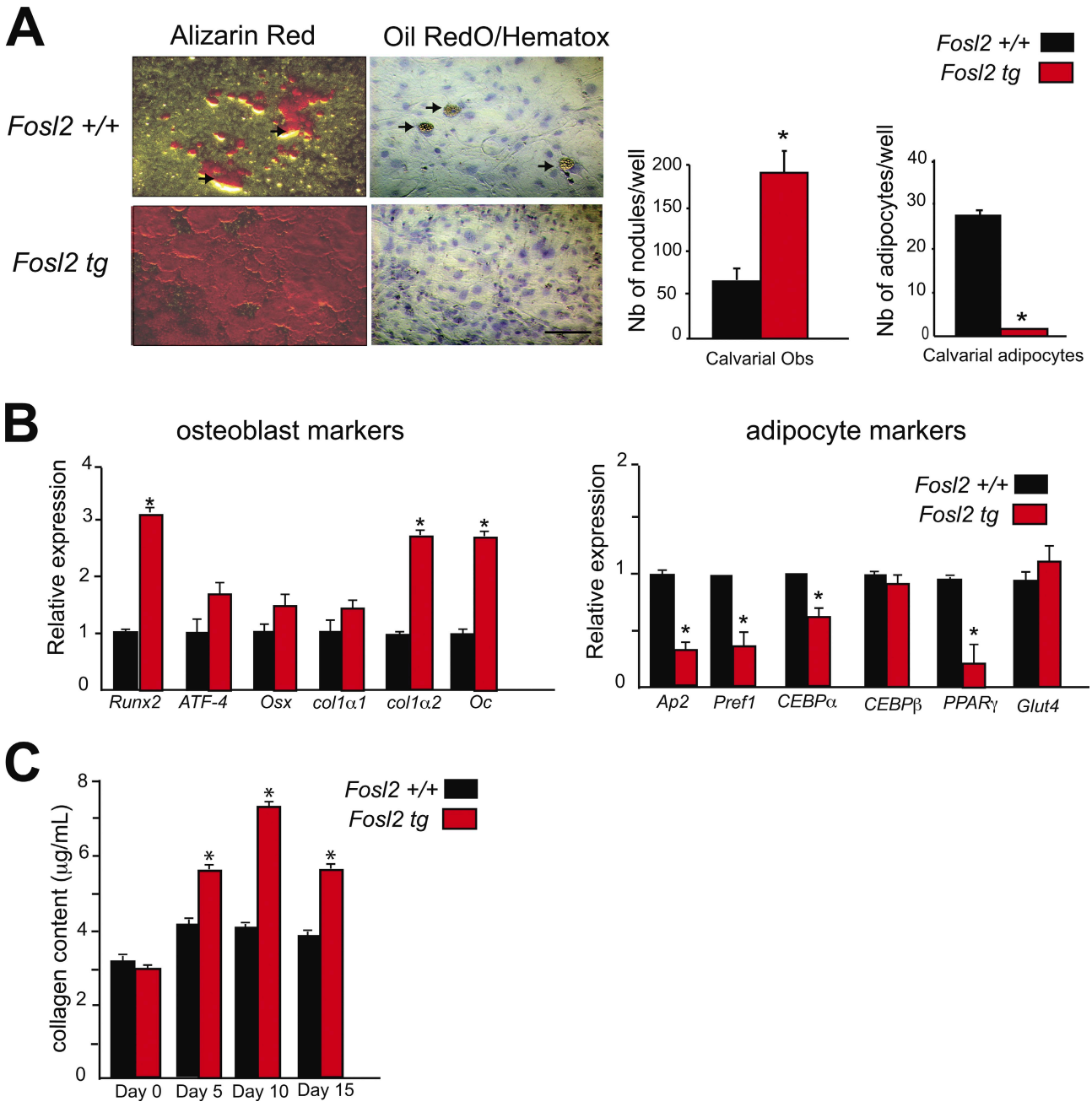

Figure 4. **Osteoblast differentiation of *Fosl2 tg* cells in vitro.** (A) Alizarin red and Oil red O/hematoxylin staining of calvaria-derived osteoblast isolated from *Fosl2*$^{+/+}$ and *Fosl2 tg* pups. Cells were cultured for 15 d on plastic in the presence of β-glycerophosphate and ascorbic acid. Quantification of the number of nodules and adipocytes per well is shown. Arrows indicate adipocytes. *n* = 3. Bar, 200 μm. (B) qPCR analyses of *Runx2*, *ATF-4*, *osterix* (*Osx*), *collagen 1α1* (*col1α1*), *collagen 1α2* (*col1α2*), and *osteocalcin* (*Oc*) in *Fosl2*$^{+/+}$ and *Fosl2 tg* cells at day 15 of differentiation (*n* = 3). Values are presented as relative expression, and wt is set to 1. (C) Collagen content in *Fosl2*$^{+/+}$ and *Fosl2 tg* osteoblast–conditioned medium at day 0, 5, 10, and 15 of differentiation (*n* = 3). Error bars represent mean values ± SD. *, P < 0.01.

reporter, suggesting that Fra-2 and ATF-4 might function as heterodimers (Fig. 5 D).

Previous studies have indicated a role for AP-1 in mediating the basal and TGF-β–induced transcription of the mouse *col1α2* gene (Chang and Goldberg, 1995), and one AP-1 binding sequence has been identified in the human *a2(I) collagen* (*COL1A2*) promoter (Chung et al., 1996). A close comparative inspection of the mouse and rat *col1α2* promoters indicated that this sequence was almost conserved at position −253 bp (proximal) and revealed two additional TRE-like elements located at positions −850 and −890 bp (distal) upstream of the transcriptional start site. A DNA fragment containing these two TRE-like elements could be specifically amplified from *Fosl2* control, but not from *Fosl2 ko* immunoprecipitates, indicating that an AP-1 complex containing Fra-2 is present on the *col1α2* promoter (Fig. 5 E). The potential Fra-2 binding partner was next investigated, and ChIP analysis of the same fragment was performed using *Fosl2* control and *ko* osteoblasts with

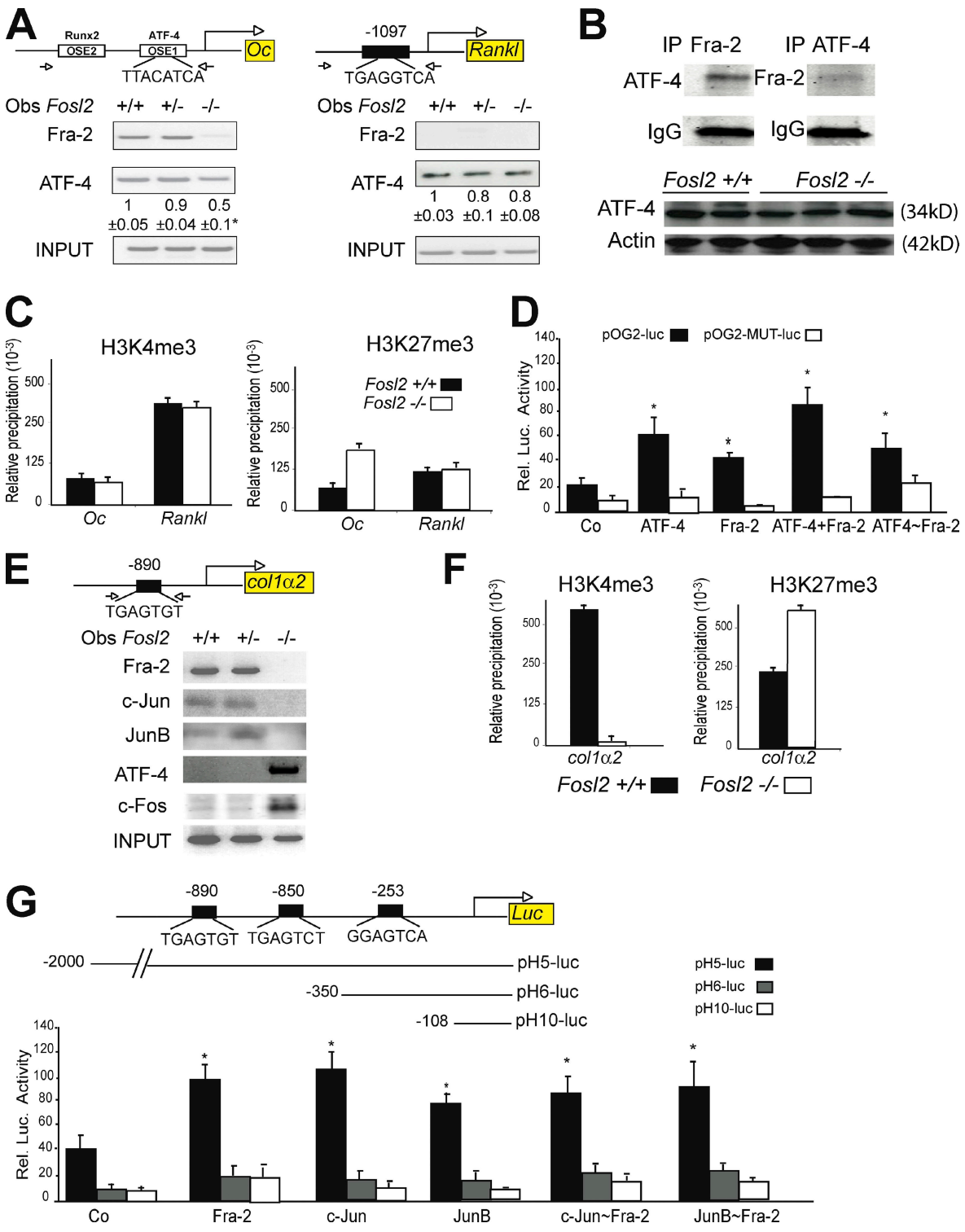

Figure 5. **Oc and col1α2 are transcriptional target genes of Fra-2.** (A) ChIP for *Oc* and *Rankl* promoter. Arrows indicate primers amplifying fragments. Chromatin of the indicated genotypes was immunoprecipitated with AP-1 antibodies. Quantification and endpoint qPCR-amplified fragments at 200 bp are shown. *, P < 0.01. (B) Coimmunoprecipitation for Fra-2 and ATF-4 in primary wt osteoblasts. IgG is used for loading control. Western blot analyses for 38 kD ATF-4 in *Fosl2*$^{+/+}$ (n = 2) and *Fosl2*$^{-/-}$ (n = 3) long bones at P2. 42 kD actin is used as loading control. (C) H3K4me3 and H3K27me3 ChIP on *Oc* and *Rankl* promoter. Chromatin from osteoblasts of the indicated genotypes was immunoprecipitated with H3K4me3- and H3K27me3-specific antibodies. Bars represent qPCR quantification relative to input chromatin. (D) wt (pOG2-luc) or Ap-1 mutated (pOG2-MUT-luc) reporter assay for the Oc promoter fragment in the presence of ATF-4, Fra-2, ATF-4 + Fra-2, and ATF-4–Fra-2 expression vectors (n = 3). (E) ChIP for col1α2 promoter. Arrows indicate primers amplifying fragments at 200 bp. Chromatin of the indicated genotypes was immunoprecipitated with AP-1 antibodies. Endpoint qPCR-amplified fragments are shown. (F) H3K4me3 and H3K27me3 ChIP on *col1α2* promoter. Chromatin from osteoblasts of the indicated genotypes was immunoprecipitated with H3K4me3- and H3K27me3-specific antibodies. Bars represent qPCR quantification relative to input chromatin. (G) pH5-luc, pH6-luc, and pH10-luc reporter assay for the *col1α2* promoter fragment in the presence of Fra-2, c-Jun, JunB, c-Jun–Fra-2, and JunB–Fra-2 expression vectors (n = 3). Error bars represent SD. *, P < 0.01.

different Jun and ATF-4 antibodies. Whereas c-Jun and JunB were clearly bound to the *col1α2* promoter in wt cells, no binding of c-Jun or JunB could be detected in the absence of Fra-2, indicating that, at least in osteoblasts, c-Jun and JunB can only bind to this putative AP-1 element as heterodimers with Fra-2. Interestingly, in the absence of Fra-2, c-Fos and ATF-4 are specifically recruited to this site (Fig. 5 E). In the *col1α2* promoter, a dramatic decrease in active (H3K4me3) methylation marks was observed in primary *Fosl2 ko* osteoblasts, which correlated with a striking increase in repressive (H3K27me3) methylation marks, indicating that in the absence of Fra-2, the *col1α2* promoter was less active (Fig. 5 F). Lastly, luciferase reporter assays using *col1α2* promoter (pH5-luc, −2,000–0 bp; pH6-luc, −350–0 bp; and pH10-luc, −108–0 bp) revealed that c-Jun, JunB, and Fra-2 expression vectors, as well as a combination of both c-Jun + Fra-2 or JunB + Fra-2, increased the activity of a pH5-luc promoter containing the −2,000–0 bp of the *col1α2* promoter (Fig. 5 G). Moreover, luciferase reporter assays performed in primary osteoblasts revealed that the increased activity observed for c-Jun, JunB, and Fra-2 expression vectors in wt cells was slightly decreased in Fra-2 knockdown osteoblasts (Fig. S2 C). ATF-4 and c-Fos expression vectors were unable to activate the *col1α2* promoter as efficiently as Fra-2 (Fig. S2 C). Forced dimers of c-Jun–Fra-2 or JunB–Fra-2 efficiently trans-activated the same reporter, suggesting that Fra-2 and c-Jun or Fra-2 and JunB were acting as heterodimers (Fig. 5 G).

These findings, together with the altered expression of *Oc* and *col1α2* observed in *Fosl2 ko* and *tg* mutants, indicate that both genes are direct transcriptional targets of Fra-2 in vivo. Fra-2–ATF-4 dimers and Fra-2 dimers with c-Jun and JunB positively regulate *Oc* and *col1α2* transcription, respectively.

Fra-2 affects matrix protein expression and osteoblast differentiation in human bone cells

To investigate the relevance of our findings to human bone cells, expression analyses of Fra-2, col1, and Oc were performed by immunohistochemistry using bone and cartilage tumor tissue arrays with unmatched normal adjacent tissues (24 cases). The normal tissue, when stained for Fra-2, col1, and Oc, revealed a common expression pattern in human stromal cells (Fig. 6 A). Moreover, Fra-2, col1, and Oc were also found expressed in stromal cells of chondroblastic Os's, osteoblastic Os's, chondrosarcomas, giant cell tumors, fibroblastic Os's, and mesenchymal chondrosarcomas (Fig. 6 A and Fig. S3 B). The localization of stromal cells was determined by hematoxylin and eosin (H&E) staining on serial sections from identical human samples (Fig. S3, A and B).

To validate these in vivo observations, the consequences of down-regulation of Fra-2 using an in vitro short hairpin RNA (shRNA) approach was analyzed in three different human Os cell lines: U2Os, sarcoma osteogenics (SAOs), and Cal72. As previously described, these cell lines have a different genetic background, including the p53 status, although all have molecular characteristics common to an osteoblastic phenotype (Rochet et al., 1999, 2003; Bruserud et al., 2005). The cell lines were differentiated into mature osteoblasts using a similar protocol to the one used for mouse primary osteoblasts. Efficient shRNA knockdown clones for Fra-2 were selected for each cell line and characterized using qPCR and Western blotting analyses (Fig. 6 B and not depicted). Importantly, all cell lines selected for shRNA control were able to differentiate into mature and functional osteoblasts as shown by Alizarin red staining (Fig. 6 B). Interestingly, decreased Fra-2 levels inhibited osteoblast differentiation in all three cell lines (Fig. 6 B). Importantly, consistent with our previous findings, Fra-2 knockdown induced adipocyte differentiation (Fig. 6 B and not depicted). In addition, *Runx2*, *col1α2*, and *Oc* mRNA levels were found to be strongly decreased in Fra-2 knockdown clones at day 15 of differentiation in all three cell lines (Fig. 6 C and not depicted), whereas *AP*, *Bsp*, and *col1α1* mRNA levels were unaffected (Fig. 6 C). The cell number of Fra-2 knockdown clones was slightly increased after 12 d in culture (Fig. 6 D). These experiments strongly support our findings in the mouse that Fra-2 expression controls osteoblast differentiation likely caused by altered expression of osteoblast-specific genes *Oc* and *col1α2* in both murine and in human cells.

Discussion

The results presented in this study reveal a novel function of Fra-2/AP-1 in skeletal biology, particularly in bone-forming osteoblasts. Mesenchyme-derived osteoblasts are responsible for extracellular matrix deposition in bone. Their activity is determined by precursor cell proliferation and differentiation and by the bone-forming activity of mature osteoblasts. Fos/AP-1 proteins, such as Fra-1 and ΔFosB, were previously found to be regulators of bone mass by affecting bone matrix production and osteoblast activity (Jochum et al., 2000; Sabatakos et al., 2000; Kveiborg et al., 2002; Eferl et al., 2004). Regarding the role of Fra-2 in skeletal biology, Fra-2 was known to regulate osteoclast formation/survival and chondrocyte differentiation (Karreth et al., 2004; Bozec et al., 2008). Here we show that Fra-2 is a key regulator in osteoblast differentiation.

The failure of Fra-2–deficient osteoblasts to mature and instead to acquire an adipogenic phenotype is remarkable. Loss of differentiation is accompanied by a decrease in expression of the osteoblast-specific *Oc* gene and reduced expression of *col1α2*. *Oc*, a γ-carboxyglutamic acid–containing noncollagenous protein, is a major component of bone extracellular matrix and is thought to be required to stimulate bone mineral maturation (Boskey, 1998). The expression of *Oc* has also been shown to be controlled by *Runx2*, an early molecular marker of the osteoblast lineage (Ducy and Karsenty, 1995; Ducy et al., 1996a). *Runx2* expression was found to be decreased in *Fosl2 ko* bones and in primary osteoblasts. However, 5 kb of promoter 1 as well as the intron1-2 defined as promoter 2 of *Runx2* were analyzed, and no binding of Fra-2 to the *Runx2* promoter could be detected by ChIP experiment (unpublished data), indicating that loss of Fra-2 likely affects *Runx2* expression indirectly. We cannot exclude that decreased *Runx2* levels contribute to impaired expression of *Oc* in cooperation with Fra-2/ATF-4. Moreover, *Runx2* could possibly affect the "switch" between osteoblasts and adipocytes in the loss-of-function experiments. *Runx2* is

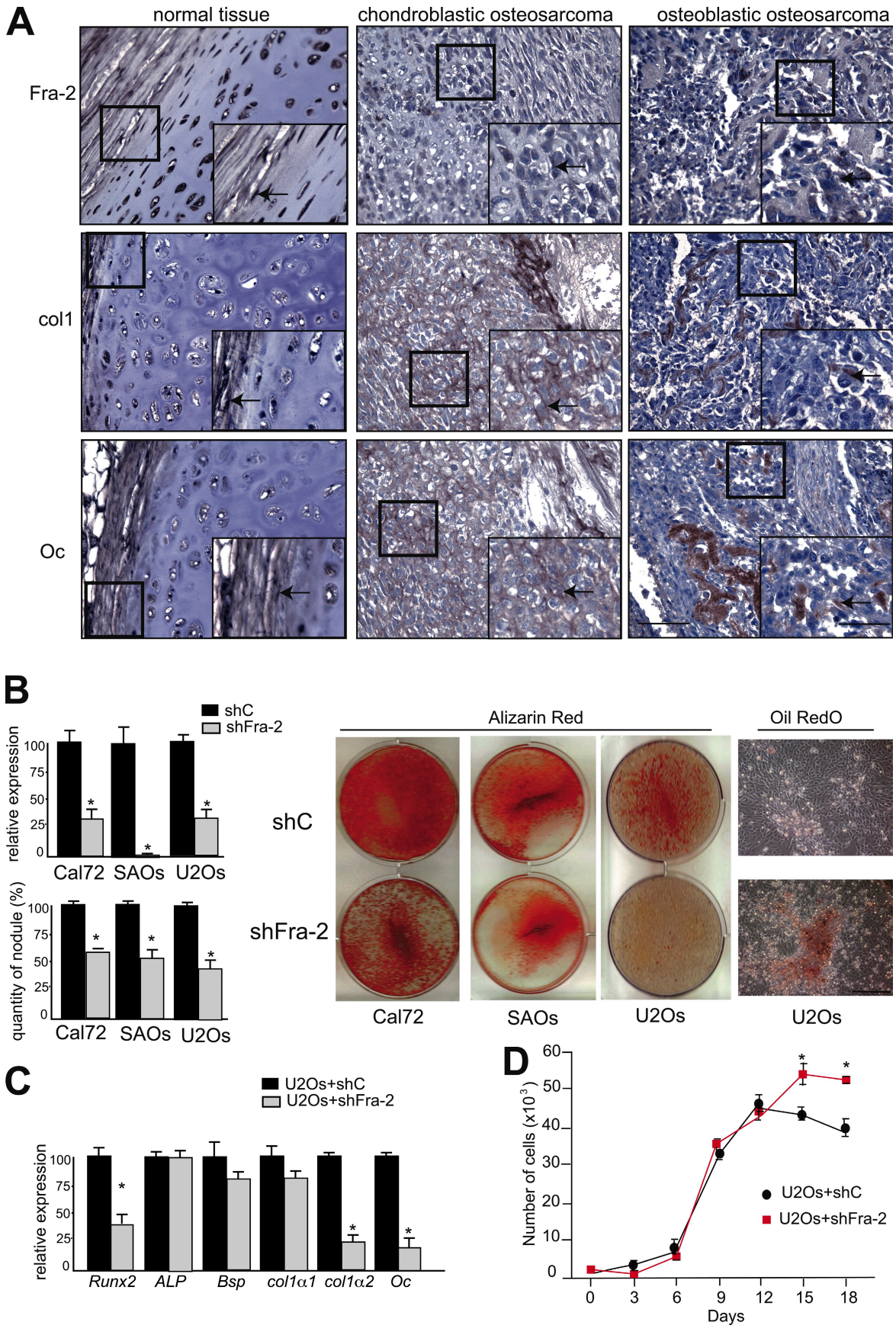
A
normal tissue
chondroblastic osteosarcoma
osteoblastic osteosarcoma
Fra-2
col1
Oc
B
shC
shFra-2
relative expression
100
75
50
25
0
*
Cal72
SAOs
U2Os
quantity of nodule (%)
Alizarin Red
Oil RedO
shC
shFra-2
Cal72
SAOs
U2Os
U2Os
C
U2Os+shC
U2Os+shFra-2
relative expression
Runx2
ALP
Bsp
col1α1
col1α2
Oc
D
Number of cells (x10^3)
60
50
40
30
20
10
0
U2Os+shC
U2Os+shFra-2
0
3
6
9
12
15
18
Days

involved in regulating the reciprocal differentiation pathway of osteoblast and adipocyte lineages. *Runx2*$^{-/-}$ osteoblasts differentiated into adipocytes at high frequency (Kobayashi et al., 2000). It is known that *Runx2* deficiency in chondrocytes causes adipogenic changes in vitro (Enomoto et al., 2004). Moreover, *PPAR-γ* can regulate *Runx2* and vice versa, although other independent pathways can regulate this factor, such as TGF-β or adipocytokines.

ATF-4, a basic leucine zipper protein capable of dimerization with Fos proteins, has been shown to be the second major determinant of osteoblast-specific expression of *Oc* (Yang et al., 2004). In this study, we demonstrate that Fra-2 dimerizes with ATF-4 to activate the *Oc* promoter in cell lines and primary osteoblasts. In the absence of Fra-2, ATF-4–containing dimers bound to the OSE1 site are greatly decreased, whereas the chromatin is enriched in inactive methylation marks. Fra-2 was not present on every ATF-4 target site, e.g., on the *Rankl* promoter, and *Rankl* expression was also not affected by loss of Fra-2. Interestingly, *Oc* expression was also found to be decreased in mice lacking JunB and Fra-1 (Eferl et al., 2004; Kenner et al., 2004). However, JunB, like Fra-1, was not able to bind to the *Oc* promoter.

Although gene deletion studies have demonstrated the importance of *Oc* in bone remodeling, *Oc* deficiency does not result in low bone mass (Ducy et al., 1996a,b). Therefore, decreased expression of *Oc* alone cannot explain the dramatic bone loss observed in Fra-2 *ko* pups. The exclusive coexpression in osteoblasts of AP, an enzyme that cleaves pyrophosphate, and col1, the most abundant and most widely distributed collagen type, is necessary and sufficient for extracellular matrix mineralization to occur in bone (Murshed et al., 2005). Col1 consists of two α1(I) chains and one α2(I) chain encoded by two different genes. We did not observe any changes in AP or in *col1α1* expression. However, there was a marked reduction of *col1α2* RNA in *Fosl2 ko* cells and a marked increase in *Fosl2 tg* long bones. The transcription of the α2(I) collagen gene involves known, but also yet to be identified, DNA sequences located in both the proximal promoter and a far upstream enhancer (Karsenty and Park, 1995). AP-1 has been implicated in the transcriptional regulation of both the mouse and the human α2(I) collagen genes by TGF-β (Chang and Goldberg, 1995; Chung et al., 1996). Fra-2 was found to bind and activate the *col1α2* promoter through a novel AP-1 binding element, and c-Jun and JunB are potential dimerization partners. Consistent with this finding, mice deficient for JunB develop a severe osteopenia with markedly reduced *col1α2* levels (Kenner et al., 2004). In addition, a recent publication has shown that TGF-β activates the human *col1α2* gene via a noncanonical signaling, which requires c-Jun or JunB transcription factor occupancies in fibroblasts (Ponticos et al., 2009). The identification of *col1α2* as a direct Fra-2/AP-1 target gene in osteoblasts establishes that AP-1 controls expression of essential extracellular matrix components. This is further substantiated by the fact that we show for the first time total collagen content of osteoblasts regulated by Fra-2.

We have recently shown that bones of Fra-2–deficient newborn mice have giant osteoclasts, and the pups are osteopenic (Bozec et al., 2008). Notably, *Opn* was found up-regulated in Fra-2 *ko* pups, which may reflect the fact that these mutants exhibit a giant osteoclast phenotype. Moreover, the data presented here strongly imply that the osteopenia is caused by a combination of cell-autonomous effects of Fra-2 on both the osteoblast and osteoclast lineages. The number and activity of osteoclasts remained unchanged in Fra-2 *tg* mice in vivo, and Rankl, OPG, as well as CTx levels in the blood were unaffected. However, increased bone resorption activity and marker gene expression were observed during osteoclast differentiation in vitro. These data suggest that Fra-2 is apparently not necessary for osteoclast differentiation in vivo and that signals from the bone surface might affect osteoclast activity, which is missing in in vitro cultures. In *Fra-1*–deficient mice, the low bone mass phenotype was reported to be a result of defects in the late maturation of osteoblasts to bone matrix–producing cells accompanied by insufficient induction of the bone matrix components *Mgp*, *Oc*, and *col1α2*. Up-regulation of *Oc* and *col1α2* expression was less pronounced in bones of Fra-1 *tg* mice compared with Mgp (Eferl et al., 2004), which is directly regulated by Fra-1 (Julien et al., 2009). In this study, we did not detect any binding of Fra-1 to the *Oc* or *col1α2* promoters, suggesting that Fra-2 might be the major AP-1 factor directly regulating this important collagen component. Moreover, Fra-2 and ΔFosB, unlike Fra-1, exert distinct effects on both osteoblastic and adipocyte differentiation in vitro (Kveiborg et al., 2002; Eferl et al., 2004). CEBP-β was found similarly regulated in ΔFosB and Fra-2 *tg* long bones. In fact, differentiation of mesenchymal cells into adipocytes involves a cascade of transcription factors, such as CEBP-β and CEBP-γ, which in turn activate PPAR-γ, an essential gene for the activation of several adipocyte-specific genes (Wu et al., 1995). Our data suggest that Fra-2 regulates adipocyte marker gene expression along with the expression of *Oc*, which is known to be important in metabolic function (Hinoi et al., 2008, 2009; Takeda and Karsenty, 2008).

Down-regulation of Fra-2 in human bone cell lines and bone tumors is accompanied by decreased osteoblast differentiation

Figure 6. **Fra-2 affects human matrix protein expression in vivo and in vitro.** (A) Immunohistochemistry for Fra-2, collagen1 (col1), and osteocalcin (Oc) in human bone normal tissue, chondrosarcoma, and osteoblastic Os. Arrows indicate Fra-2, col1, or Oc-positive staining for stromal cells in human bone sample. Bar, 100 µm. Inset bar, 50 µm. (B) qPCR analyses of Fra-2 at day 0 of differentiation in Cal72, SAOs, and U2Os human Os cell clones. Area of nodule formation quantification where shRNA control clones represent 100%. $n = 3$. Alizarin red staining (Cal72, SAOs, and U2Os) and Oil red O (U2Os) staining of control and Fra-2 knockdown human Os cells. Cells were cultured for 15 d on plastic in the presence of β-glycerophosphate and ascorbic acid. (C) qPCR analyses of osteoblast markers *Runx2*, *AP*, *bone sialoprotein* (*Bsp*), *collagen 1α1* (*colα1*), *collagen 1α2* (*col1α2*), and *Oc* at day 15 of differentiation. Values are presented as relative expression, and wt is set to 100. (D) Cumulative cell number (proliferation) of U2Os shRNA control and U2Os shRNA Fra-2 clones. Error bars represent mean values ± SD. *, $P < 0.01$.

with a switch to adipogenesis. This implies that the underlying molecular mechanism is conserved between mice and humans. The relevance of these findings for osteoporosis and human bone mass regulation is supported by preliminary data demonstrating coexpression and possible coregulation of Fra-2, Oc, and col1 in human Os's of osteoblastic and chondrogenic origin, both in vivo and in vitro. Chondroblastic Os is the most common primary malignancy of the skeleton and comprises ~25% of all cases of Os (Li and Siegal, 2010). Because treatment and prognosis are very different for chondroblastic Os's compared with giant cell tumors of bone, it is important to have a reliable assay to distinguish between these different bone tumors (Fox et al., 2009). Although our results are preliminary, we would like to suggest that coexpression of Fra-2, col1, and Oc in certain Os's might possibly be used as a diagnostic tool. In summary, this study has identified Fra-2 as a novel regulator of bone matrix production and osteoblast differentiation, which presents a novel paradigm to modulate bone mass and could be considered for the development of future therapeutic strategies for diseases involving bone loss.

Materials and methods

Mice and tissue fixation
The generation of *Fosl2*$^{-/-}$ and *Fosl2 tg* mice has been described previously (Eferl et al., 2007, 2008). All mice were maintained on a mixed C57BL6/129 background.

RNA isolation and reverse transcription
Total RNA was isolated with the TRIZOL protocol (Invitrogen). cDNA synthesis was performed using 2 µg RNA with the Ready To Go You Prime It First-Strand Beads and random primers (GE Healthcare) according to the manufacturer's protocols.

Histological analysis and histomorphometry
Mice were killed by CO_2 asphyxia, and bones were fixed in 3.7% PBS-buffered formaldehyde. For histological and in situ hybridization analysis, bones were embedded in paraffin. For histomorphometrical analysis, undecalcified tibiae and lumbar spines were embedded in methylmethacrylate, and 5-µm sections were cut in the sagittal plane. Sections were stained with toluidine blue and modified von Kossa/van Gieson. Quantitative histomorphometry was performed on toluidine blue–stained sections according to standardized protocols (Parfitt et al., 1987) using the Osteomeasure histomorphometry system (Osteometrix). Experiments were performed in a blinded fashion.

In situ hybridization and immunohistochemistry
Immunohistochemistry stainings for Fra-2 (Abcam), col1 (Santa Cruz Biotechnology, Inc.), and Oc (Santa Cruz Biotechnology, Inc.) were performed on deparaffinized sections using the labeled streptavidin-biotin or Envision detection kit (Dako). For in situ hybridization, digoxigenin-labeled riboprobes were synthesized according to the manufacturer's instructions (DIG RNA labeling kit; Boehringer Ingelheim). The signal was detected using BM purple–AP-substrate solution according to the manufacturer's (Boehringer Ingelheim) instructions. Sections were then washed, fixed in 4% PFA, and mounted. Pictures were taken using a microscope (DM3000; Leica) with 40x (oil; NA 1.25–0.75), 20x (no medium; NA 0.70), and 10x (no medium; NA 0.15) objectives (Plan Apochromat) outfitted with a charge-coupled device camera at a temperature of 24°C and Leica Application Suite Image Acquisition and Analysis software.

Osteoblast and osteoclast cultures
Calvariae were sequentially digested for 10 min in modified MEM type α containing 0.1% collagenase and 0.2% dispase. Cells isolated by fractions 2–3 were combined as an osteoblastic cell population, expanded for 2 d in MEM type α with 10% FCS, and replated at a density of 5×10^5 cells/well, and medium was supplemented with 10 mM β-glycerophosphate and 50 µg/ml ascorbic acid (Eferl et al., 2004). After 3 wk of culture, bone nodules were identified by Alizarin S red staining (Sigma-Aldrich), and adipocytes were identified by Oil red O staining.

Bone marrow cells were isolated from 6-wk-old mice, brought into suspension overnight, and then cultured in 24 wells at a density of 5×10^5 cells/well, 20 ng/ml macrophage colony–stimulating factor (R&D Systems), and 5 ng/ml Rankl (R&D Systems) for 2–7 d.

Real-time PCR analyses
qPCR reactions were performed using SYBR green (Invitrogen) on an Opticon2 Monitor Fluorescence Thermocycler (MJ Research). The comparative CT method was used to quantify the amplified fragments. RNA expression levels were normalized to at least one housekeeping gene (*tubulin*, *actin*, and *hprt*), whereas chromatin-bound fragments were normalized to the same fragments amplified from input chromatin.

CTx measurements
CTx levels were determined in sera from mice fasting for 4 h before bleeding using a commercial kit (RatsLap; Immunodiagnostic).

Collagen content
Collagen contents were analyzed in conditioned medium during osteoblast differentiation using the Sircoll procedure following the Sircoll kit instructions from Biocolor.

shRNA experiments
shRNA for Fra-2 and control (random sequence) virus were generated following the protocol from Sigma-Aldrich (Mission RNA). Primary or osteoblast cell lines were infected with the virus. shRNA knockdown clones for Fra-2 were selected for each cell line by puromycin and characterized by qPCR and Western blotting.

ChIP
ChIP was performed according to standard protocols with antibodies against Fra-2, Fra-1, c-Fos, JunB, JunD, c-Jun, ATF-4 (Santa Cruz Biotechnology, Inc.), K4 (Millipore), and K27 (gift from T. Jenuwein). The specific binding of each Jun and Fos antibody was verified in parallel using a corresponding pair of *wt* and *ko* osteoblasts and the *Fosl1* canonical TRE element as a target sequence. Bound and unbound fragments were quantified by real-time PCR.

Reporter assay
The promoter–reporter vectors for Oc and col1α2 were gifts of G. Karsenty and B. de Combrugghe, respectively (Goldberg et al., 1992; Ducy et al., 1996b). 6×10^4 Cos7 cells/well were plated in 24-well dishes. 1.5 µg of the luciferase reporter construct, 0.2 µg of the renilla internal control (pHRG-tk; Promega), and 0.2–1 µg of each AP-1 expression vector were cotransfected in triplicate using calcium phosphate (Bakiri et al., 2002). JunB–Fra-2, cJun–Fra-2, and ATF-4–Fra-2 forced dimer constructs were generated as previously described (Bakiri et al., 2002). Luciferase activity was quantified using the Dual Luciferase kit (Promega).

Statistical analysis
All experiments were repeated at least three times and done in triplicate. Statistical analysis was performed using a *t* test. $P < 0.01$ was accepted as significant. Data are shown as means, and the error bars represent SD.

Online supplemental material
Fig. S1 shows the osteoclast phenotype in *Fosl2 tg* mice. Fig. S2 shows that col1α2 and Oc are direct transcriptional targets of Fra-2 in primary osteoblasts. Fig. S3 shows Fra-2 and matrix protein expression in human samples. Online supplemental material is available at http://www.jcb.org/cgi/content/full/jcb.201002111/DC1.

We are very grateful to Drs. A.E. Grigoriadis, J.P. David, and Ö. Uluckan for critically reading the manuscript and for helpful comments. We also thank G. Karsenty for providing the Oc promoter and ATF-4 expression constructs, B. de Crombrugghe for providing col1 expression constructs, and T. Jenuwein for methyl histone antibodies. Many thanks also to A. Höbertz for her initial analyses of Fra-2 *ko* pups and expert help.

This work was supported in part by the European Union (Molecular Mechanisms of Bone Formation and Anabolism grant to E.F. Wagner). A. Bozec was funded by the European Calcified Tissue Society, and E.F. Wagner was funded by a European Research Council Advanced grant (ERC FCK/2008/37).

Submitted: 19 February 2010
Accepted: 7 August 2010

References

Bakiri, L., K. Matsuo, M. Wisniewska, E.F. Wagner, and M. Yaniv. 2002. Promoter specificity and biological activity of tethered AP-1 dimers. *Mol. Cell. Biol.* 22:4952–4964. doi:10.1128/MCB.22.13.4952-4964.2002

Behrens, A., J. Haigh, F. Mechta-Grigoriou, A. Nagy, M. Yaniv, and E.F. Wagner. 2003. Impaired intervertebral disc formation in the absence of Jun. *Development.* 130:103–109. doi:10.1242/dev.00186

Boskey, A.L. 1998. Biomineralization: conflicts, challenges, and opportunities. *J. Cell. Biochem. Suppl.* 72:83–91. doi:10.1002/(SICI)1097-4644(1998)72:30/31+<83::AID-JCB12>3.0.CO;2-F

Bozec, A., L. Bakiri, A. Hoebertz, R. Eferl, A.F. Schilling, V. Komnenovic, H. Scheuch, M. Priemel, C.L. Stewart, M. Amling, and E.F. Wagner. 2008. Osteoclast size is controlled by Fra-2 through LIF/LIF-receptor signalling and hypoxia. *Nature.* 454:221–225. doi:10.1038/nature07019

Bruserud, O., K.J. Tronstad, and R. Berge. 2005. In vitro culture of human osteosarcoma cell lines: a comparison of functional characteristics for cell lines cultured in medium without and with fetal calf serum. *J. Cancer Res. Clin. Oncol.* 131:377–384. doi:10.1007/s00432-004-0650-z

Chang, E., and H. Goldberg. 1995. Requirements for transforming growth factor-beta regulation of the pro-alpha 2(I) collagen and plasminogen activator inhibitor-1 promoters. *J. Biol. Chem.* 270:4473–4477. doi:10.1074/jbc.270.9.4473

Chien, K.R., and G. Karsenty. 2005. Longevity and lineages: toward the integrative biology of degenerative diseases in heart, muscle, and bone. *Cell.* 120:533–544. doi:10.1016/j.cell.2005.02.006

Chung, K.Y., A. Agarwal, J. Uitto, and A. Mauviel. 1996. An AP-1 binding sequence is essential for regulation of the human alpha2(I) collagen (COL1A2) promoter activity by transforming growth factor-beta. *J. Biol. Chem.* 271:3272–3278. doi:10.1074/jbc.271.6.3272

David, J.P., K. Sabapathy, O. Hoffmann, M.H. Idarraga, and E.F. Wagner. 2002. JNK1 modulates osteoclastogenesis through both c-Jun phosphorylation-dependent and -independent mechanisms. *J. Cell Sci.* 115:4317–4325. doi:10.1242/jcs.00082

Ducy, P., and G. Karsenty. 1995. Two distinct osteoblast-specific cis-acting elements control expression of a mouse osteocalcin gene. *Mol. Cell. Biol.* 15:1858–1869.

Ducy, P., C. Desbois, B. Boyce, G. Pinero, B. Story, C. Dunstan, E. Smith, J. Bonadio, S. Goldstein, C. Gundberg, et al. 1996a. Increased bone formation in osteocalcin-deficient mice. *Nature.* 382:448–452. doi:10.1038/382448a0

Ducy, P., V. Geoffroy, and G. Karsenty. 1996b. Study of osteoblast-specific expression of one mouse osteocalcin gene: characterization of the factor binding to OSE2. *Connect. Tissue Res.* 35:7–14. doi:10.3109/03008209609029169

Eferl, R., A. Hoebertz, A.F. Schilling, M. Rath, F. Karreth, L. Kenner, M. Amling, and E.F. Wagner. 2004. The Fos-related antigen Fra-1 is an activator of bone matrix formation. *EMBO J.* 23:2789–2799. doi:10.1038/sj.emboj.7600282

Eferl, R., R. Zenz, H.C. Theussl, and E.F. Wagner. 2007. Simultaneous generation of fra-2 conditional and fra-2 knock-out mice. *Genesis.* 45:447–451. doi:10.1002/dvg.20311

Eferl, R., P. Hasselblatt, M. Rath, H. Popper, R. Zenz, V. Komnenovic, M.H. Idarraga, L. Kenner, and E.F. Wagner. 2008. Development of pulmonary fibrosis through a pathway involving the transcription factor Fra-2/AP-1. *Proc. Natl. Acad. Sci. USA.* 105:10525–10530. doi:10.1073/pnas.0801414105

Elefteriou, F., J.D. Ahn, S. Takeda, M. Starbuck, X. Yang, X. Liu, H. Kondo, W.G. Richards, T.W. Bannon, M. Noda, et al. 2005. Leptin regulation of bone resorption by the sympathetic nervous system and CART. *Nature.* 434:514–520. doi:10.1038/nature03398

Enomoto, H., T. Furuichi, A. Zanma, K. Yamana, C. Yoshida, S. Sumitani, H. Yamamoto, M. Enomoto-Iwamoto, M. Iwamoto, and T. Komori. 2004. Runx2 deficiency in chondrocytes causes adipogenic changes in vitro. *J. Cell Sci.* 117:417–425. doi:10.1242/jcs.00866

Fox, C., Z.S. Husain, M.B. Shah, D.R. Lucas, and H.A. Saleh. 2009. Chondroblastic osteosarcoma of the cuboid: a literature review and report of a rare case. *J. Foot Ankle Surg.* 48:388–393. doi:10.1053/j.jfas.2009.02.004

Goldberg, H., T. Helaakoski, L.A. Garrett, G. Karsenty, A. Pellegrino, G. Lozano, S. Maity, and B. de Crombrugghe. 1992. Tissue-specific expression of the mouse alpha 2(I) collagen promoter. Studies in transgenic mice and in tissue culture cells. *J. Biol. Chem.* 267:19622–19630.

Grigoriadis, A.E., K. Schellander, Z.Q. Wang, and E.F. Wagner. 1993. Osteoblasts are target cells for transformation in c-fos transgenic mice. *J. Cell Biol.* 122:685–701. doi:10.1083/jcb.122.3.685

Hinoi, E., N. Gao, D.Y. Jung, V. Yadav, T. Yoshizawa, M.G. Myers Jr., S.C. Chua Jr., J.K. Kim, K.H. Kaestner, and G. Karsenty. 2008. The sympathetic tone mediates leptin's inhibition of insulin secretion by modulating osteocalcin bioactivity. *J. Cell Biol.* 183:1235–1242. doi:10.1083/jcb.200809113

Hinoi, E., N. Gao, D.Y. Jung, V. Yadav, T. Yoshizawa, D. Kajimura, M.G. Myers Jr., S.C. Chua Jr., Q. Wang, J.K. Kim, et al. 2009. An Osteoblast-dependent mechanism contributes to the leptin regulation of insulin secretion. *Ann. NY Acad. Sci.* 1173(Suppl 1):E20–E30. doi:10.1111/j.1749-6632.2009.05061.x

Jochum, W., J.P. David, C. Elliott, A. Wutz, H. Plenk Jr., K. Matsuo, and E.F. Wagner. 2000. Increased bone formation and osteosclerosis in mice overexpressing the transcription factor Fra-1. *Nat. Med.* 6:980–984. doi:10.1038/79676

Julien, M., S. Khoshniat, A. Lacreusette, M. Gatius, A. Bozec, E.F. Wagner, Y. Wittrant, M. Masson, P. Weiss, L. Beck, et al. 2009. Phosphate-dependent regulation of MGP in osteoblasts: role of ERK1/2 and Fra-1. *J. Bone Miner. Res.* 24:1856–1868. doi:10.1359/jbmr.090508

Karreth, F., A. Hoebertz, H. Scheuch, R. Eferl, and E.F. Wagner. 2004. The AP1 transcription factor Fra2 is required for efficient cartilage development. *Development.* 131:5717–5725. doi:10.1242/dev.01414

Karsenty, G., and R.W. Park. 1995. Regulation of type I collagen genes expression. *Int. Rev. Immunol.* 12:177–185. doi:10.3109/08830189509056711

Karsenty, G., and E.F. Wagner. 2002. Reaching a genetic and molecular understanding of skeletal development. *Dev. Cell.* 2:389–406. doi:10.1016/S1534-5807(02)00157-0

Kawamata, A., Y. Izu, H. Yokoyama, T. Amagasa, E.F. Wagner, K. Nakashima, Y. Ezura, T. Hayata, and M. Noda. 2008. JunD suppresses bone formation and contributes to low bone mass induced by estrogen depletion. *J. Cell. Biochem.* 103:1037–1045. doi:10.1002/jcb.21660

Kenner, L., A. Hoebertz, T. Beil, N. Keon, F. Karreth, R. Eferl, H. Scheuch, A. Szremska, M. Amling, M. Schorpp-Kistner, et al. 2004. Mice lacking JunB are osteopenic due to cell-autonomous osteoblast and osteoclast defects. *J. Cell Biol.* 164:613–623. doi:10.1083/jcb.200308155

Kobayashi, H., Y. Gao, C. Ueta, A. Yamaguchi, and T. Komori. 2000. Multilineage differentiation of Cbfa1-deficient calvarial cells in vitro. *Biochem. Biophys. Res. Commun.* 273:630–636. doi:10.1006/bbrc.2000.2981

Kveiborg, M., R. Chiusaroli, N.A. Sims, M. Wu, G. Sabatakos, W.C. Horne, and R. Baron. 2002. The increased bone mass in deltaFosB transgenic mice is independent of circulating leptin levels. *Endocrinology.* 143:4304–4309. doi:10.1210/en.2002-220420

Li, S., and G.P. Siegal. 2010. Small cell tumors of bone. *Adv. Anat. Pathol.* 17:1–11.

Murshed, M., D. Harmey, J.L. Millán, M.D. McKee, and G. Karsenty. 2005. Unique coexpression in osteoblasts of broadly expressed genes accounts for the spatial restriction of ECM mineralization to bone. *Genes Dev.* 19:1093–1104. doi:10.1101/gad.1276205

Parfitt, A.M., M.K. Drezner, F.H. Glorieux, J.A. Kanis, H. Malluche, P.J. Meunier, S.M. Ott, and R.R. Recker. 1987. Bone histomorphometry: standardization of nomenclature, symbols, and units. Report of the ASBMR Histomorphometry Nomenclature Committee. *J. Bone Miner. Res.* 2:595–610. doi:10.1002/jbmr.5650020617

Ponticos, M., C. Harvey, T. Ikeda, D. Abraham, and G. Bou-Gharios. 2009. JunB mediates enhancer/promoter activity of COL1A2 following TGF-beta induction. *Nucleic Acids Res.* 37:5378–5389. doi:10.1093/nar/gkp544

Reimold, A.M., M.J. Grusby, B. Kosaras, J.W. Fries, R. Mori, S. Maniwa, I.M. Clauss, T. Collins, R.L. Sidman, M.J. Glimcher, and L.H. Glimcher. 1996. Chondrodysplasia and neurological abnormalities in ATF-2-deficient mice. *Nature.* 379:262–265. doi:10.1038/379262a0

Rochet, N., J. Dubousset, C. Mazeau, E. Zanghellini, M.F. Farges, H.S. de Novion, A. Chompret, B. Delpech, N. Cattan, M. Frenay, and J. Gioanni. 1999. Establishment, characterisation and partial cytokine expression profile of a new human osteosarcoma cell line (CAL 72). *Int. J. Cancer.* 82:282–285. doi:10.1002/(SICI)1097-0215(19990719)82:2<282::AID-IJC20>3.0.CO;2-R

Rochet, N., P. Leroy, D.F. Far, L. Ollier, A. Loubat, and B. Rossi. 2003. CAL72: a human osteosarcoma cell line with unique effects on hematopoietic cells. *Eur. J. Haematol.* 70:43–52. doi:10.1034/j.1600-0609.2003.02766.x

Rodan, G.A., and T.J. Martin. 2000. Therapeutic approaches to bone diseases. *Science.* 289:1508–1514. doi:10.1126/science.289.5484.1508

Sabatakos, G., N.A. Sims, J. Chen, K. Aoki, M.B. Kelz, M. Amling, Y. Bouali, K. Mukhopadhyay, K. Ford, E.J. Nestler, and R. Baron. 2000. Overexpression of DeltaFosB transcription factor(s) increases bone formation and inhibits adipogenesis. *Nat. Med.* 6:985–990. doi:10.1038/79683

Takeda, S., and G. Karsenty. 2008. Molecular bases of the sympathetic regulation of bone mass. *Bone.* 42:837–840. doi:10.1016/j.bone.2008.01.005

Teitelbaum, S.L., and F.P. Ross. 2003. Genetic regulation of osteoclast development and function. *Nat. Rev. Genet.* 4:638–649. doi:10.1038/nrg1122

Wagner, E.F., and R. Eferl. 2005. Fos/AP-1 proteins in bone and the immune system. *Immunol. Rev.* 208:126–140. doi:10.1111/j.0105-2896.2005.00332.x

Wu, Z., Y. Xie, N.L. Bucher, and S.R. Farmer. 1995. Conditional ectopic expression of C/EBP beta in NIH-3T3 cells induces PPAR gamma and stimulates adipogenesis. *Genes Dev.* 9:2350–2363. doi:10.1101/gad.9.19.2350

Yang, X., K. Matsuda, P. Bialek, S. Jacquot, H.C. Masuoka, T. Schinke, L. Li, S. Brancorsini, P. Sassone-Corsi, T.M. Townes, et al. 2004. ATF4 is a substrate of RSK2 and an essential regulator of osteoblast biology; implication for Coffin-Lowry Syndrome. *Cell.* 117:387–398. doi:10.1016/S0092-8674(04)00344-7